PHILOSOPHICAL TRANSACTIONS OF THE ROYAL SOCIETY A MATHEMATICAL, PHYSICAL & ENGINEERING SCIENCES

Oxygen in Pore Waters of Deep-Sea Sediments [and Discussion]

M. M. Rutgers Van Der Loeff, P. S. Meadows and J. A. Allen

Phil. Trans. R. Soc. Lond. A 1990 **331**, 69-84
doi: 10.1098/rsta.1990.0057

Phil. Trans. R. Soc. Lond. A **331**, 69–84 (1990) [69]
Printed in Great Britain

Oxygen in pore waters of deep-sea sediments

By M. M. Rutgers van der Loeff†
Netherlands Institute for Sea Research, P.O. Box 59, *NL* 1790 *AB Den Burg, The Netherlands*

Profiles of dissolved oxygen are presented from contrasting ocean areas, and compared with data on the distribution of trace elements in sediment and pore water. The release of manganese starts when oxygen is depleted to about 1 μM. In the Sulu Sea (Philippines), the manganese flux to this interface balanced $48 \pm 16\,\%$ of the oxygen flux. Large excess O_2 fluxes in the east Atlantic are attributed to non-steady-state diagenesis. At the transition from O_2 to manganese reduction, cobalt and nickel are mobilized, and many trace elements, including rare earth elements, undergo a phase transition as a result of the dissolution of the manganese oxyhydroxide carrier phase.

In the deep Angola Basin, Weddell Sea and west equatorial Pacific, oxygen penetrates the sediment to well over 1 m. In the semi-enclosed Sulu Sea with a low oxygen concentration in the bottom water ($O_{bw} = 55$ μM), z_o increases from 1 cm at 1000 m water depth to 10–15 cm at 4000 m, and decreases again to 1 cm in the deepest spots covered by turbidites. Generally, the depth where oxygen is depleted (z_o) increases with increasing water depth; z_o decreases at the approach of the continent and under the influence of turbidites; it increases at topographic highs exposed to winnowing.

A model is presented that relates z_o to O_{bw}, primary production and water depth. z_o is especially sensitive to changes in organic matter input and O_{bw} when oxygen breaks through the bioturbated zone. The large differences in z_o at the same water depth in the Sulu Sea and adjacent South China Sea and west equatorial Pacific (6, 14 and 40 cm at 3500 m depth) can be explained merely by the differences in O_{bw} (55, 105 and 150 μM respectively). It is concluded that glacial to interglacial changes in O_{bw} must have had major effects on diagenesis and infauna throughout the world oceans.

Introduction

The flux of oxygen to depths below the reactive surface layer represents only a minor fraction of the total mineralization, but is of major importance for the diagenetic behaviour of trace elements. As oxygen inhibits the use of other electron acceptors, the onset of manganese and NO_3 reduction – and all chemical changes associated with these redox transitions – is controlled by the penetration of oxygen in the sediment.

This controlling role of oxygen can in principle be studied through measurements of the vertical distributions of dissolved oxygen and of dissolved and particulate trace elements in the same cores. Coastal sediments are not suitable for such a study, because oxygen is depleted here at a depth of only a few millimeters. High-precision oxygen profiles have been measured with microelectrodes (Revsbech *et al.* 1980), but all gradients are so steep that it is very hard to measure trace element concentration profiles with sufficient resolution. Moreover, bioturbation and the occurrence of microenvironments ensure that the various reactions that would

† Present address: Alfred Wegener Institute for Polar and Marine Research, Columbusstrasse, D-2850 Bremerhaven, F.R.G.

thermodynamically be predicted to occur sequentially, are often in fact not separated in space in distinct depth horizons (see, for example, Aller 1988).

In the deep sea the supply rate of organic matter and all reaction rates are much lower. As a result oxygen penetrates much deeper into the sediment, and all pore water gradients can be well resolved. Such sediments offer a good opportunity to study the distribution of both oxygen and trace elements around the depth of oxygen depletion.

Data on dissolved oxygen distributions in deep-sea sediments below the reactive surface layer (Reimers *et al.* 1984; Reimers 1987) are scarce. Murray & Grundmanis (1980) showed that oxygen concentrations level off at non-zero values in carbonate oozes of the central equatorial Pacific. In the eastern equatorial Pacific, oxygen penetrates to about 5 cm in a carbonate ooze and to over 20 cm in a siliceous ooze (Jahnke *et al.* 1982; Reimers *et al.* 1984). In a carbonate ooze in the Cape Verde abyssal plain, half of the bottom-water oxygen remains at 1 m depth, and little consumption occurs between 1–2 m (Sørensen & Wilson 1984; Wilson *et al.* 1985). The same authors showed that at a station in the Madeira abyssal plain, a buried turbidite caused oxygen to be depleted at about 40 cm depth.

Only Wilson *et al.* (1985, 1986) and Wallace *et al.* (1988), who studied deep-sea sediments in which the oxygen-oxidation front is moving downward, give data on the distribution of both oxygen and of some trace elements around the depth of oxygen depletion. Thus, most studies on early diagenesis and redox behaviour of trace elements in deep-sea sediments did not include measurements of dissolved oxygen, but had to infer the oxygen distribution from manganese, NO_3 and Eh data (Froelich *et al.* 1979; Klinkhammer 1980; Klinkhammer *et al.* 1982; Hartmann & Müller 1982; Müller *et al.* 1988) or calcium and alkalinity data (Sayles 1981).

This paper gives distributions of dissolved oxygen in deep-sea sediments from the Pacific, Atlantic and Southern Ocean. Data from the semi-enclosed Sulu Sea (Philippines) and adjacent South China Sea and western equatorial Pacific allow a comparison of basins whose bottom waters differ strongly in ventilation and consequently in the oxygen content in their bottom waters. The balance of diffusive fluxes at the transition from oxygen to manganese reduction is compared with existing models. The distribution of some trace elements in sediment and pore water above and below this transition is shown to illustrate the influence of the transition on the chemical environment in the sediment.

It is concluded that the depth z_o, where the transition from oxygen to manganese respiration takes place, is of major importance for the diagenetic development of the sediment. A model is developed to investigate the dependence of z_o on primary production, water depth and the oxygen concentration in the bottom water.

Material and methods

Station locations are listed in table 1. Samples from the Angola Basin were collected with R. V. *Tyro* in 1980 with a 5.5 cm diameter gravity corer. Bennekom & Berger (1984) have reported pore-water silicate data from these cores. Samples from a northeastern Atlantic site were obtained during two expeditions, one in 1982 with R. V. *Tyro* and one in 1984 with H. Ms. *Tydeman*. The sedimentology, biology and hydrography of this site, which has been used for the disposal of radioactive waste, has been studied in detail (NEA 1985; Rutgers van der Loeff & Lavaleye 1986). The latter reference gives a more elaborate account of sampling methods as well as stratigraphic and other additional data of the cores described here. Box-cores

Table 1. Position and water depth of sediment cores

core number	position		depth/m	core number	position		depth/m
Angola Basin				Sulu Sea			
T80-21	16° 45′ S	6° 28′ E	5400	MW 8	8° 8.5′ N	118° 35.0′ E	1005
T80-25	33° 29′ S	5° 33.5′ W	4235	MW 9	8° 20.1′ N	118° 57.0′ E	1995
T80-27	35° 51′ S	6° 44′ W	4325	MW 10	8° 20.6′ N	118° 57.6′ E	1980
T80-28	32° 38′ S	8° 27.5′ W	4295	MW 11	8° 8.1′ N	118° 34.8′ E	1020
T80-29	25° 17.5′ S	6° 57′ W	5015	MW 12	8° 2.9′ N	118° 22.4′ E	510
T80-30	18° 40′ S	5° 10′ W	5180	MW 13	8° 16.1′ N	118° 51.7′ E	1515
T80-33	0° 36′ S	13° 8′ W	4360	MW 14	6° 54.5′ N	119° 10.2′ E	2995
T80-34	0° 52′ N	14° 7′ W	4195	MW 15	7° 33.9′ N	120° 29.8′ E	3995
T80-35	0° 28′ N	14° 20′ W	4505	MW 16	7° 32.9′ N	120° 19.5′ E	4000
				MW 17	7° 25.7′ N	121° 10.3′ E	4455
northeastern Atlantic				MW 18	7° 25.3′ N	121° 12.5′ E	4515
T82-11G	46° 0.9′ N	17° 7.9′ W	4725	MW 19	7° 10.6′ N	119° 29.9′ E	3533
T82-15G	45° 54.9′ N	16° 31.5′ W	4000	MW 20	6° 54.5′ N	119° 10.0′ E	3000
T84-21B	47° 03.2′ N	14° 57.8′ W	4787	MW 21	6° 46.4′ N	118° 58.0′ E	2400
T84-25B	46° 05.6′ N	16° 42.0′ W	4723				
T84-25G	46° 05.1′ N	16° 44.3′ W	4675	South China Sea			
T84-27G	45° 57.3′ N	17° 11.8′ W	4720	MW 2	12° 7.2′ N	118° 3.7′ E	2950
T84-29Gb	46° 04.8′ N	16° 56.2′ W	4430	MW 3	10° 57.3′ N	118° 27.6′ E	1095
				MW 4	11° 53.3′ N	118° 30.5′ E	2150
Weddell Sea				MW 6	7° 43.0′ N	116° 22.9′ E	993
PS 1485-1	72° 33.5′ S	18° 47.4′ W	2075				
PS 1490-2	74° 40.7′ S	35° 5.2′ W	487	western equatorial Pacific			
PS 1498-1	73° 29.2′ S	35° 31.9′ W	2825	MW 22	7° 18.6′ N	138° 11.0′ E	3515
PS 1507-2	68° 37.8′ S	20° 3.5′ W	4771	MW 23	7° 37.1′ N	138° 47.7′ E	3025

from the Weddell Sea were taken during the ANT V/4 expedition (1987) with R. V. *Polarstern*. Data are presented of four cores along a gradient from the shelf to the deep Weddell Sea. In the Sulu Sea and adjacent South China Sea and western equatorial Pacific Ocean, a Soutar boxcorer was used during an expedition with R. V. *Moana Wave* in 1988.

All operations on freshly collected cores (electrode measurements and pore water collection) were done in a refrigerated laboratory kept at about sea-floor temperature (2 °C; in the Sulu Sea: 10 °C).

Dissolved oxygen measurements

In the northeastern Atlantic and the Angola Basin, oxygen was measured on cores inside a nitrogen-filled glove bag. When the core had cooled to about 6 °C, about 1 h after retrieval, sediment samples were taken with 10 cm^3 polypropylene syringes with the tops cut off. Dissolved oxygen was determined by flushing the electrode of a Radiometer blood gas analyser with wet sediment from the syringes. The active surface of the electrode was 20 μm in diameter, and the readings were stable after 3 min, during which fresh sediment was flushed a few times over the electrode. Calibration proceeded with nitrogen gas and air, and was checked with Winkler titration in bottom-water samples. Measurements of a sediment sample that was brought into gas exchange equilibrium with a bottom-water sample proved that porosity had a negligible effect on the oxygen readings.

In the Weddell Sea and Sulu Sea, oxygen was measured with a minielectrode (Helder & Bakker 1985), mounted in a polypropylene pipette, to allow insertion to the required depth in the sediment. These commercial electrodes have a high stirring effect (i_∞/i_0 up to 1.6, Gust *et al.* (1987)), and their response in the sediment is reduced by the reduced diffusivity (cf. Revsbech 1989).

In analogy to Gust *et al.* (1987), the oxygen flux J from the pore water to the electrode surface, with concentrations C_w and C_i respectively, is

$$J = k_s(C_w - C_i) = k_{wo}(C_w - C_i)/F,$$

where k_s and k_{wo} are the mass transport coefficient in the pore water and overlying water respectively, and F is the formation factor. In analogy to (A 8) in Gust *et al.* (1987) it can be shown that

$$i_s = i_\infty/(1 + (k_m/k_{wo})\,F),$$

and with (A 8)
$$i_s/i_0 = (1 + ((i_\infty/i_0) - 1))/(1 + F((i_\infty/i_0) - 1)), \quad (1)$$

where i_s is the current in the sediment, i_0 is the current in stagnant water and i_∞ is the current at infinite mixing rate.

The Weddell Sea measurements were corrected with this formula. The data in the Sulu Sea were obtained with an electrode with a thicker membrane, which reduced the output current to about 300 pA at air saturation, and a correction according to equation (1) (up to 5% at 10 cm depth) was not applied. Calibration was done against Winkler titration in bottom-water samples. Profiles measured from the top or the bottom of a subcore were in good agreement (e.g. PS 1498, figure 6).

Pore water analyses

Pore water was collected by squeezing or (Sulu Sea) centrifuging and subsequent filtration. No precautions were taken to exclude contact of boxcore samples with atmospheric oxygen. Segments of gravity cores were transferred into a nitrogen-filled glove bag, where sediment from selected depth horizons was filled into squeezers. The first 2 cm^3 was discarded. In subsequent aliquots, nutrients were analysed with standard autoanalyser techniques and alkalinity by potentiometric titration. All equipment that came into contact with samples for trace metal analyses had been thoroughly rinsed in 6 M hydrochloric acid and double distilled water before use. Trace metal contents in samples acidified with 1 cm^3 per litre of 6 M HCl suprapur were determined by flameless atomic absorption spectroscopy (AAS) using direct injection for manganese and a preconcentration for iron, cobalt and nickel (Danielsson *et al.* 1979). Blanks run through all procedures, including filtration in the teflon squeezers on board, were 2, 25, 0.05 and 0.3 nmol kg^{-1} respectively.

Formation factor was measured according to Andrews & Bennett (1981). Details on sediment analyses have been given elsewhere (Rutgers van der Loeff & Lavaleye 1986). Shortly, the selective extraction procedure (modified after Lyle *et al.* (1984)) distinguishes four phases: HAC, soluble in acetic acid and acetate buffer pH 5; HAM, reducible in hydroxylammonium chloride and citrate buffer pH 5; HCl, soluble in 1 M HCl; and a residual phase.

Results

Dissolved oxygen profiles

Sediments in the central Angola Basin (stations to the left in figure 1) are oxygenated throughout. The oxygen concentration levels off at about half the bottom-water value. At the approach of the continent the supply of organic matter and consequently the consumption of oxygen increases. At station 33 there is just enough organic material to deplete oxygen at

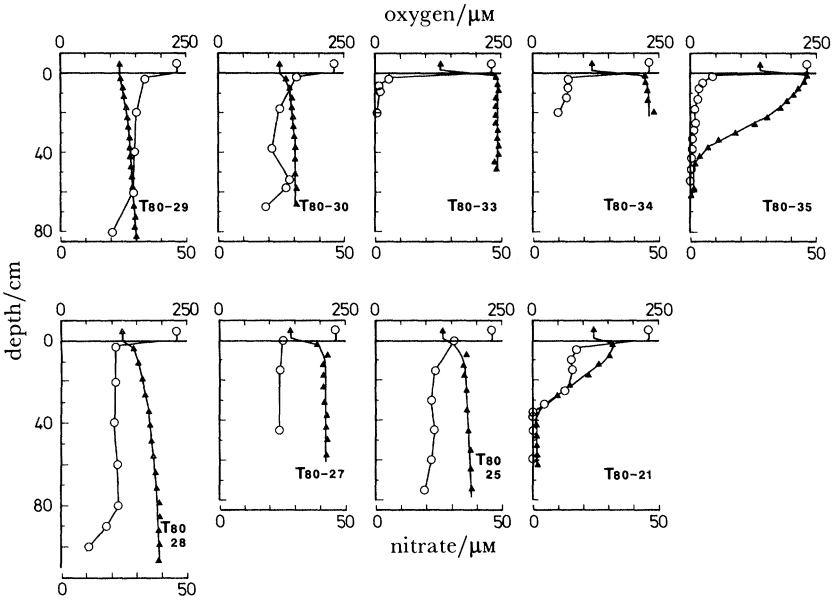

FIGURE 1. Depth profiles of dissolved oxygen (○) and nitrate (▲) concentrations in the pore water of cores from the Angola Basin, with, to the right, decreasing distance to the continent.

25 cm, but not enough to continue with nitrate respiration. At stations 21 and 35 mineralization continues with nitrate respiration. This latter core is comparable with the cores from the Romanche Fracture Zone area studied by Froelich *et al.* (1979). From nitrate and dissolved manganese data these authors inferred an oxygen penetration to 20–45 cm in cores outside 300 km offshore. At their station located 200 km offshore, manganese reduction started at 8–12 cm. In comparing actual gradients we should consider that core shortening (Lebel *et al.* 1982) increased the gradients in our 5.5 cm diameter cores by a factor of 2 (van Bennekom & Berger 1984), whereas this effect is smaller in the 6.7 cm diameter cores of Froelich *et al.* Near the continental slope the sediments become increasingly reduced. In the slope sediments off West Africa oxygen must be depleted very close to the sediment–water interface, as judged from published sulphate, alkalinity, ammonia and manganese data (Hartmann *et al.* 1976; Suess 1976).

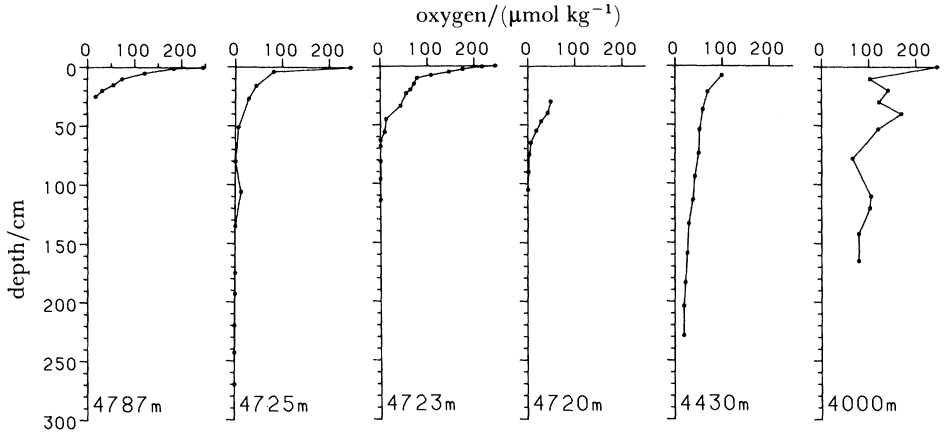

FIGURE 2. Depth profiles of dissolved oxygen concentrations in the pore water of cores from the northeastern Atlantic, in order of decreasing water depth. From left to right the core numbers are 21B, 11G, 25B+G, 27G, 29Gb and 15G.

In the deeper parts of the northeastern Atlantic site, oxygen is depleted at a depth of 60–100 cm (figure 2). At slopes and topographic highs cores up to 2.5 m in length were entirely oxygenated. In the Porcupine abyssal plain oxygen is nearly depleted at 25–30 cm (station T84-21B in figure 2; station T82-1B in Rutgers van der Loeff & Lavaleye (1986)).

In the central Weddell Sea (core PS 1507) dissolved oxygen stabilizes at about 100 μM below 10 cm (figure 6), and must be present to at least several metres depth. A high oxygenation is in agreement with the extremely low particle rain rate as observed with a sediment trap (Fischer *et al.* 1988). The oxygen penetration depth shallows towards the shelf, and on the shelf the oxygenated zone is limited to only a few cm (additional cores are reported in Rutgers van der Loeff & van Bennekom (1989)).

The relation between water depth and oxygen penetration is particularly well illustrated by the data from a transect in the Sulu Sea (figure 7).

Transition metals

The suboxic release of manganese is observed in all cores where the oxygen depletion depth is reached. (Manganese was not measured in the cores from the Angola Basin.) The distribution of transition metals around the oxic–suboxic transition was studied in detail in cores T82-11 (figure 3) and T84-25 (figures 4 and 5) from the northeastern Atlantic site. The vertical resolution and data quality of the upper 22 cm of core T84-25G was improved by the use of boxcore samples. The results of the boxcore (0–22 cm) and the gravity core (28–250 cm) are presented together in figures 4 and 5. Although these cores (T84-25B and T84-25G) were collected about 3 km apart, the sediment and pore water data fit very well into a single set of profiles. This combination of profiles from two different cores is moreover justified by the observation that gradients of dissolved oxygen and nutrients are very similar in boxcores collected at approximately the same depth in the area (Rutgers van der Loeff & Lavaleye 1986). The near-surface maxima in particulate manganese, cobalt and nickel in figure 5 result from the expression of the data on a carbonate-free basis, and are thus related to the strong gradient of $CaCO_3$ content with depth in the sediment from 88 % at the surface to 32 % at 1 m depth. The low trace metal contents in the sediment at 55 and 105 cm result from dilution with i.a. quartz and dolomite, minerals with low trace metal contents, by ice-rafting (Rutgers van der Loeff & Lavaleye 1986).

The manganese and iron data for pore water and sediment fit well with established models. Reduction of manganese in the suboxic sediment followed by upward diffusion and reoxidation causes the well-known accumulation of manganese in the sediment in the aerobic zone (figure 5; Lynn & Bonatti 1965; Froelich *et al.* 1979; Burdige & Gieskes 1983). Iron exhibits a similar redox behaviour, although the resulting fluxes do not cause an equally significant accumulation in the oxic layer. A colour transition at 61 cm marked the Fe^{III}–Fe^{II} transition (Lyle 1983). An enrichment of iron at the glacial to Holocene transition (Wilson *et al.* 1985; Wallace *et al.* 1988) was not observed. The elevated iron and manganese concentrations at greater depth indicate that sulphate reduction is of minor importance in this core, in agreement with the low alkalinity values and the lack of a smell of H_2S.

The diagenetic behaviour of cobalt is very similar to that of manganese, in agreement with the few available literature data on cobalt concentrations in pore waters of coastal (Martin 1985; Sundby *et al.* 1986) and deep-sea (Heggie & Lewis 1984) sediments. As in the water column, the concentrations of iron, manganese and cobalt are very low in the pore water of oxic

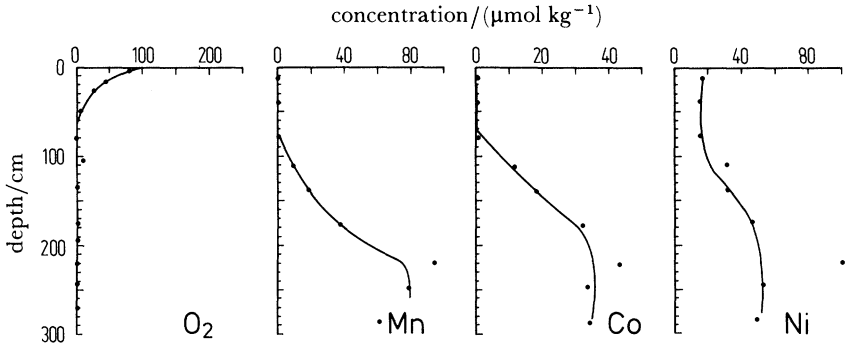

FIGURE 3. Depth profiles of oxygen and transition metals concentrations in the pore water of core T82-11G.

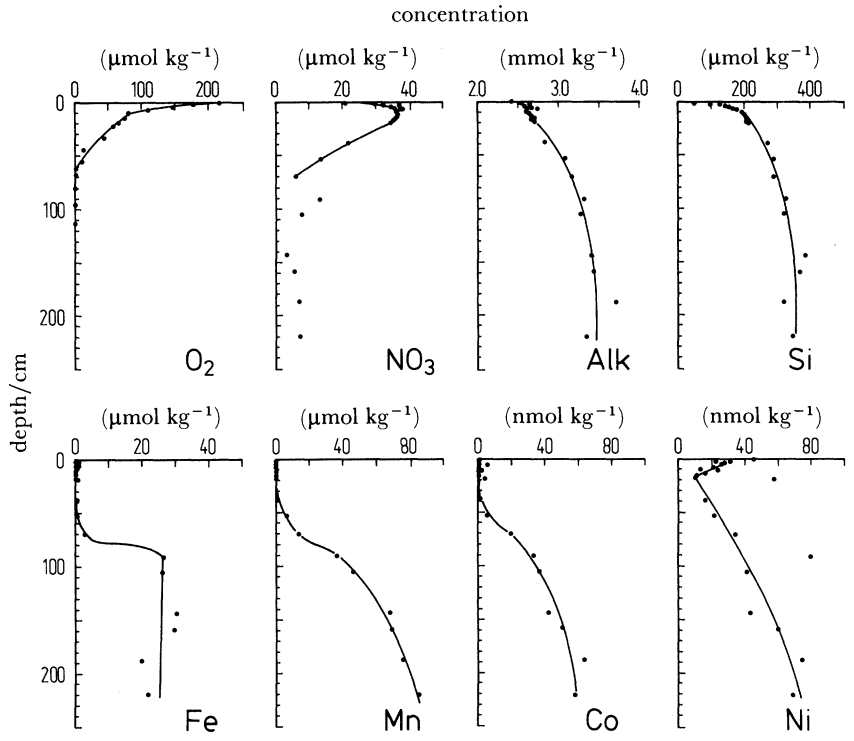

FIGURE 4. Depth profiles of oxygen, nitrate, alkalinity, silicate and transition metals concentrations in the pore water of core T84-25(B+G).

sediments. In the suboxic sediment, pore water concentrations increase sharply with depth. As with manganese, cobalt is enriched in the sediment in the oxic layer in agreement with Heggie & Lewis (1984) and Gendron *et al.* (1986). Manganese, cobalt and also nickel occur here predominantly in the HAM-reducible extract, corresponding to the manganese oxyhydroxide phase, whereas the much smaller amounts in the reduced layer occur in the HAC extract (manganese probably as mixed carbonate overgrowths on Foraminifera tests (Boyle 1983)) and in the HCl extract (cobalt and nickel).

Nickel is released by oxic mineralization of organic matter in the surface sediment (Klinkhammer *et al.* 1982; Westerlund *et al.* 1986; Heggie *et al.* 1986). The nickel profile in figure 4 suggests that nickel is readsorbed below the surface in the aerobic layer, as has been

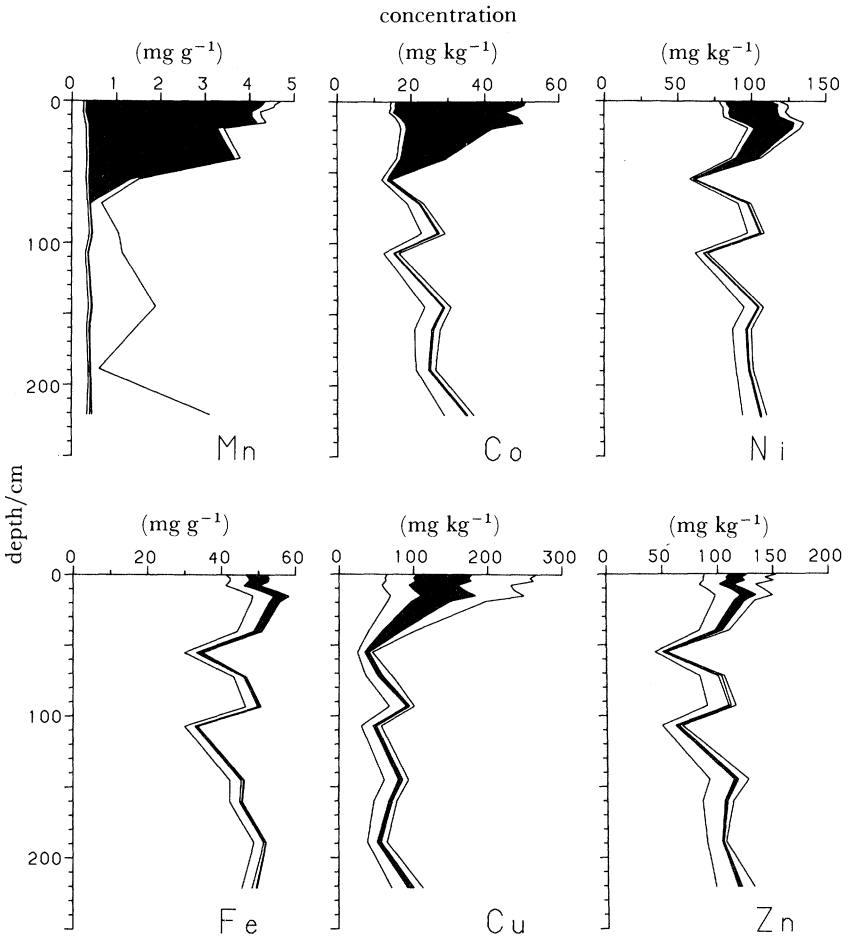

FIGURE 5. Partitioning of transition metals in the sediment of core T84-25(B+G), expressed on a $CaCO_3$-free basis. Total amounts utmost right lines, and from right to left the amounts remaining after HAC, HAM, and HCl extracts. Area representing HAM (reducible) extract is black.

shown for copper (Callender & Bowser 1980; Klinkhammer *et al.* 1982). In the suboxic layer, the concentration of dissolved nickel increases again with depth, resulting in an upward diffusive flux. Nickel is strongly enriched in the reducible phase of the oxic sediment, and its behaviour is thus similar to that of manganese and cobalt. An upward diffusive flux of nickel associated with the manganese redox pump has been demonstrated previously by Klinkhammer (1980). The accumulation of copper and zinc in the reducible phase of the oxic sediment is less pronounced, and resembles more the behaviour of iron.

DISCUSSION

The sequence of electron acceptors

Thermodynamics predict that electron acceptors are used in the order $O_2 > NO_3 = Mn > Fe > SO_4$. The order in which NO_3 and manganese are used depends on the mineral form in which Mn^{IV} occurs (Froelich *et al.* 1979). The data of Froelich *et al.* indicated that Mn is reduced before nitrate. The present data (figures 3–7 and 9) confirm that manganese reduction

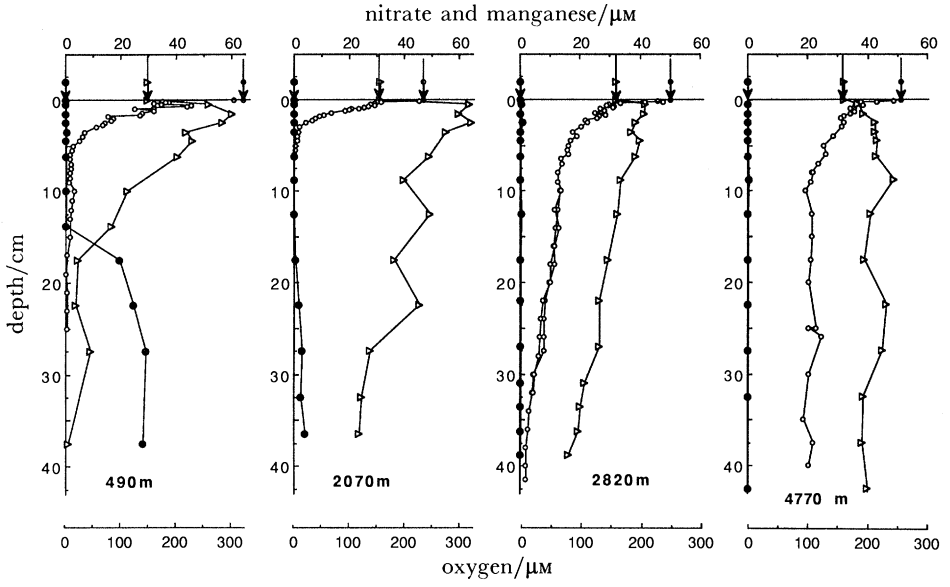

FIGURE 6. Depth profiles of oxygen (○), nitrate (▷) and manganese (●) concentrations in the pore water of four cores from the Weddell Sea, in order of increasing water depth. From left to right the core numbers are PS 1490, 1485, 1498 and 1507.

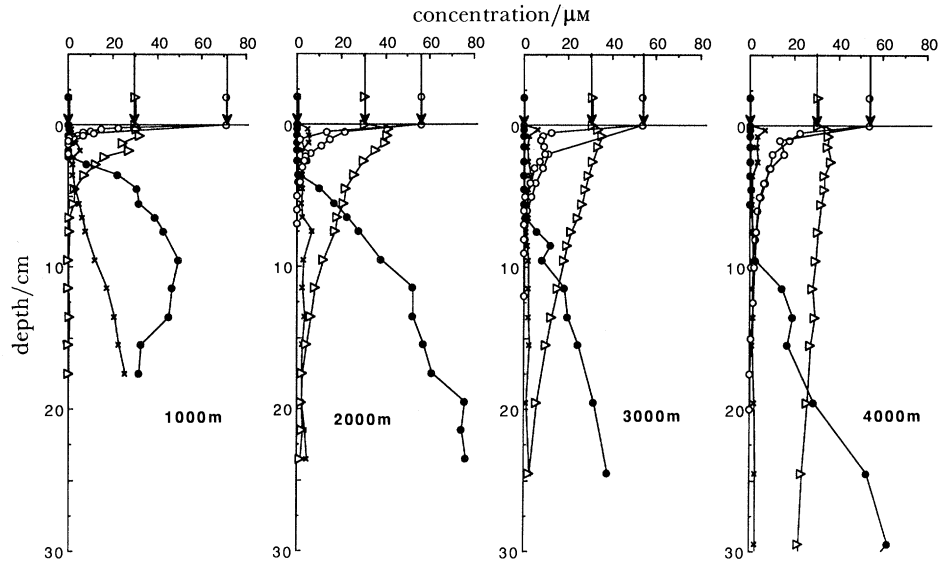

FIGURE 7. Depth profiles of oxygen (○), nitrate (▷), manganese (●) and ammonia (×) concentrations in the pore water of four cores from the Sulu Sea, in order of increasing water depth. From left to right the core numbers are MW 11, 9, 20 and 16.

starts immediately below the depletion of molecular oxygen. This justifies the separation of the sediment in an oxic and a suboxic zone, where 'oxic' implies the presence of dissolved oxygen and 'suboxic' the absence of dissolved oxygen (i.e. less than about 1 μM) and the presence of reduced manganese.

The oxygen–manganese interface

In steady state, the diffusive flux of oxygen towards this interface should be balanced by upward fluxes of reductants, of which Mn^{2+}, Fe^{2+}, S^{2-} and NH_4^+ are considered here. Fluxes of

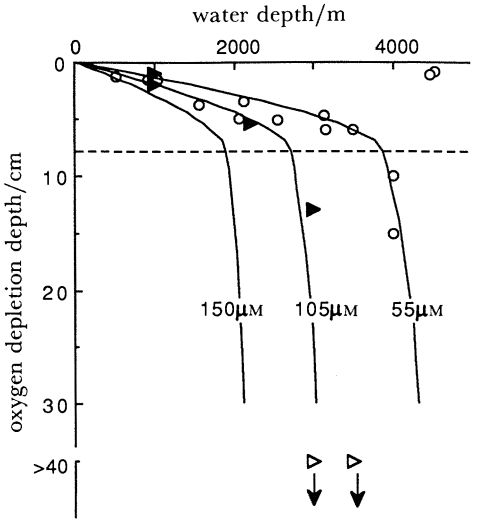

FIGURE 8. Depth of the transition from oxygen to manganese respiration in cores from the Sulu Sea (○), the South China Sea (▶) and the western equatorial Pacific (▷), compared with the model predictions for the respective concentrations of oxygen in the bottom waters of these basins (55, 105 and 150 μM). D_s corrected for porosity using $D_s = \phi^2 D$, and for temperature (10.5, 2, and 2 °C). $z_b = 8$ cm (broken line). Other parameters: $C_{prod} = 50$ g C m^{-2} a^{-1} (from the table in Suess 1980); $\beta = 0.31$ cm^{-1} (cf. Emerson *et al.* 1985); $\omega = 4$ cm ka^{-1}; $r = 0.01$ (Müller *et al.* 1988); k_2 (s^{-1}) $= 5.7 \times 10^{-8}\ \omega^{1.47}$ (Müller & Mangini 1980); $\phi = 0.8$.

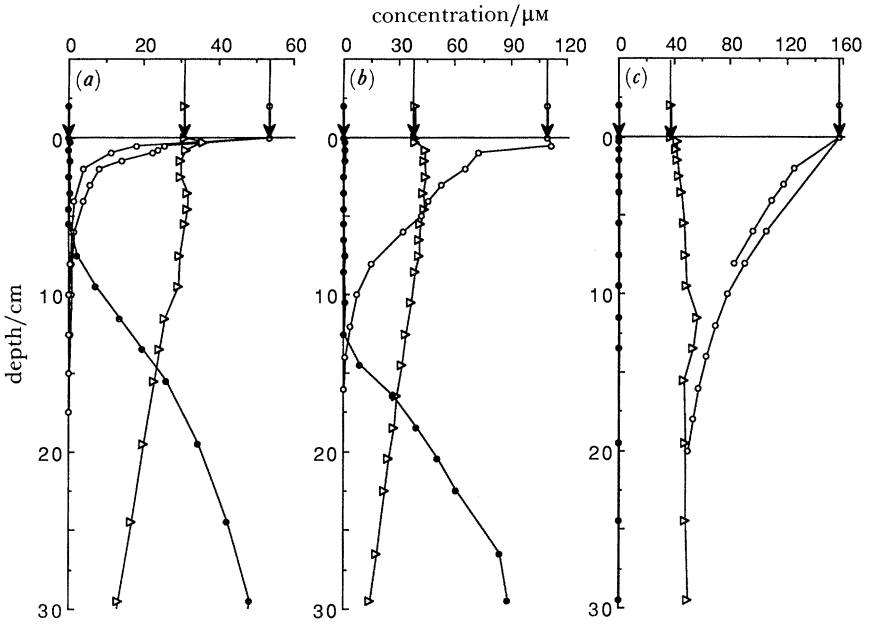

FIGURE 9. Depth profiles of oxygen (○), nitrate (▷) and manganese (●) concentrations in the pore water of sediments at comparable water depth in (*a*) the Sulu Sea ($O_{bw} = 55$ μM, 3550 m), (*b*) the South China Sea ($O_{bw} = 105$ μM, 3000 m) and (*c*) the western equatorial Pacific ($O_{bw} = 150$ μM, 3500 m).

reduced trace elements as Co^{II}, liberated together with manganese, are insignificant compared with the manganese flux. The reduction of iron and sulphate starts below the reduction of manganese and nitrate (see, for example, Froelich *et al.* 1979) and it is assumed here that upward fluxes of Fe^{2+} and S^{2-} are oxidized by nitrate and Mn^{4+}, and do not reach the oxic–suboxic interface.

Froelich *et al.* supposed that at the oxic–suboxic interface the upward flux of manganese is balanced by a downward flux of oxygen. This hypothesis can be tested with the present data. From the observed concentration gradients of oxygen, manganese and ammonia, diffusive fluxes can be derived when due account is given to the respective diffusivities. If it is assumed that ammonia and Mn^{2+} are oxidized to nitrate and MnO_2, an oxygen concentration gradient of 1 μM cm^{-1} balances concentration gradients of manganese or ammonia of 6.8 and 0.6 μM cm^{-1} respectively. In nine cores from the Sulu Sea, the manganese flux to the interface is balanced by $48 \pm 16\%$ of the O_2 flux. The remaining half may be used for oxidation of ammonia. Significant ammonia gradients were only observed in shallow cores: in core MW 11 (1000 m depth, figure 7) the ammonia and manganese fluxes have indeed a comparable oxygen demand. In the deep Sulu Sea with much weaker gradients in dissolved manganese, the required ammonia concentration gradients of only 0.1–0.3 μM cm^{-1} might have remained undetected.

In cores T82-11 and T84-25, the manganese flux accounts for only 16% and 7% respectively of the oxygen flux to the interface, leaving a large excess oxygen flux. An excess oxygen flux develops when the input of organic matter to the surface sediment is reduced, and it results in a downward migration of the oxidation front (Wilson *et al.* 1985). Such a non-steady-state situation is a likely explanation for the non-reactive zones that were concluded by Froelich *et al.* (1979) and Goloway & Bender (1982) from linear parts in their nitrate profiles. Non-steady-state diagenesis has also been invoked by Pedersen *et al.* (1986) to reconcile profiles of dissolved and particulate manganese that do not display the expected manganese accumulation at the base of the oxic zone. Rather, they found particulate manganese concentrations decreasing with depth in the oxic zone, and argued that this profile had not yet adjusted to a recent drop in input of organic carbon.

In the northeastern Atlantic cores reported here, the entire oxic sediment layer is enriched in manganese and in the elements cobalt and nickel that follow its diagenetic behaviour. There is no indication of burial of a bed with high organic carbon content, or of the formation of iron-rich bands, which results from the adjustment of the sediment to a change in organic input (Wilson *et al.* 1985). It will be shown below that the steady-state penetration depth of oxygen in the sediment is very sensitive to changes in the input of organic matter. Small variations in the rain rate of organic material to the sediment are sufficient for the oxidation front to move up and down over the course of time. Variations on a timescale long enough compared with the establishment of a diagenetic manganese signal result in multiple peaks (Berger *et al.* 1983); more rapid variations (timescale in the order of 100 years, or shorter in the example of Pedersen *et al.*) and bioturbation may explain the more homogeneous enrichment observed in core T84-25.

Manganese oxyhydroxide as carrier phase of trace elements

Trace element distributions in pore water and in the sediment show a dramatic change in sediment chemistry at the transition from oxygen to manganese reduction. The behaviour of iron and manganese is explained by the transition of these metals between oxidation states of highly different solubilities. $Ce^{IV}O_2$ (DeBaar 1988) and cobalt, which is adsorbed as Co^{III} on MnO_2 surfaces in the aerobic sediment (Murray & Dillard 1979), are similarly reduced in anoxic waters to more soluble forms. Other elements, like nickel, copper, zinc (figures 3–5) are affected indirectly by the dissolution of manganese and iron oxyhydroxides. In the oxic sediment, these hydrous oxides offer strong adsorption sites. All adsorbed elements must be

released upon the reductive dissolution of this phase, followed either by an increased mobility or a readsorption to a different phase.

The mobilization of trivalent rare earth elements (REE) in anoxic waters (DeBaar 1988) and pore waters (Elderfield & Sholkovitz 1987) was explained as such an indirect effect. A passive change in phase distribution of trivalent REE as a result of the dissolution of manganese oxyhydroxides in the sediment of core T84-25 was shown elsewhere (Rutgers van der Loeff & Lavaleye 1986).

Whether the mechanism is direct or indirect, the onset of the sudden change in mobility and phase distribution of a range of elements is entirely controlled by the depth at which oxygen is depleted. This stresses the value of a model to predict this depth from local sedimentary and hydrographical conditions.

A model for the depth of oxygen penetration

Oxygen is depleted when its consumption for the oxidation of organic matter and of other reduced substances diffusing from below exceeds the supply by diffusion from the bottom water. The consumption is determined by the supply of organic material to the ocean floor. Based on published sediment trap data, Suess (1980) has given an empirical relation between the carbon flux F_c, the primary production rate of organic carbon (C_{prod}) and water depth Z_w (m):

$$F_c(Z_w) = C_{prod}/(0.0238Z_w + 0.212). \tag{2}$$

Emerson *et al.* (1985) presented a model describing the dynamics of oxygen and carbon in a bioturbated deep-sea sediment. They derived a relation between the depth of oxygen depletion z_o and the bioturbation rate K ($cm^2\ s^{-1}$), the organic carbon decomposition rate k (s^{-1}), the oxygen concentration in the bottom water O_{bw} (moles cm^{-3}), and the organic carbon flux at the interface F_c (moles $cm^{-2}\ s^{-1}$)

$$\frac{e^{\beta z_o} + e^{-\beta z_o} - 2}{e^{\beta z_o} - e^{-\beta z_o}} = \frac{\phi O_{bw} D_s \beta \gamma}{F_c}, \tag{3}$$

where $\beta = \sqrt{(k/K)}$ and $\gamma = 106/138$, the stoichiometric ratio of moles carbon oxidized to moles oxygen reduced. Although not explicitly stated, this equation is based on the boundary condition that the oxygen flux is zero at the depth where oxygen is depleted, i.e. the consumption of oxygen for the oxidation of reductants diffusing from below is neglected.

Combining equations (2) and (3), and solving for z_o,

$$z_o = \beta^{-1} \ln [(Q+1)/(1-Q)], \tag{4}$$

where $Q = \phi O_{bw} D_s \beta \gamma (0.0238Z_w + 0.212)/C_{prod}$.

Equation (4) was derived for a bioturbated sediment. When oxygen penetrates below the bioturbated zone (thickness z_b), this model is no longer valid. It can, however, be expanded by a zone $z > z_b$ where carbon is only transported by sediment accumulation ω. The first-order carbon degradation rate (k_2) is substantially reduced in this layer. In analogy with a 2-G model (cf. Berner 1980), it will further be assumed that a part (r) of the organic supply is resistant to decomposition in the bioturbated layer, and is only decomposed below z_b at the reduced rate. This gives rise to a resistant carbon concentration of rF_c/ω in the bioturbated zone: carbon, bulk (in mol cm^{-3}),

$$0 < z < z_b, \quad K\,\partial^2 C/\partial z^2 - k(C - (rF_c/\omega)) = 0,$$

$$z > z_b, \quad \omega\,\partial C/\partial z = k_2 C = 0,$$

where the boundary conditions are; at

$$z = 0, \quad -K\,\partial C/\partial z = F_c\,(1-r),$$

at $$z = z_b, \quad -K\,\partial C/\partial z = C\omega,$$

oxygen, $$0 < z < z_b, \quad \phi D_s\,\partial^2 O/\partial z^2 - (k/\gamma)\,(C - (rF_c/\omega)) = 0,$$

$$z > z_b, \quad \phi D_s\,\partial^2 O/\partial z^2 - (k_2/\gamma)\,C = 0,$$

where the boundary conditions are; at

$$z = 0, \quad O = O_{bw},$$

at $$z = z_b, \quad (\partial O/\partial z)_{z<z_b} = (\partial O/\partial z)_{z>z_b}, \quad O_{z<z_b} = O_{z>z_b},$$

at $$z = z_o, \quad O = 0, \quad \partial O/\partial z = 0$$

(again neglecting oxidation of upward diffusing substances) with the solutions:

$0 < z < z_b$

$$C = A\,e^{\beta z} + B\,e^{-\beta z} + (rF_c/\omega),$$

$$O = (k/\beta^2\phi D_s\gamma)\,(A\,e^{\beta z} + B\,e^{-\beta z} - A - B) + O_{bw} + Dz,$$

$z > z_b$

$$C = C_{z_b}\exp\,(-k_2(z-z_b)/\omega),$$

$$O = \frac{\omega^2 C_{z_b}}{k_2\gamma\phi D_s}\exp\,(-k_2(z-z_b)/\omega) + Fz + E,$$

where

$$A = \frac{-F_c(1-r)/K\beta}{\exp\,(2\beta z_b(\omega + K\beta)/(\omega - K\beta)) + 1},$$

$$B = A + F_c(1-r)/K\beta,$$

$$D = \frac{\omega C_{z_b}}{\gamma\phi D_s}\exp\,(-k_2(z_o - z_b)/\omega).$$

$$E = \frac{-\omega C_{z_b}}{\gamma\phi D_s}\exp\,(-k_2(z_o - z_b)/\omega)\,(z_o + \omega/k_2),$$

$$F = D + (rF_c/\gamma\phi D_s),$$

and $C_{z_b} = C$ at depth z_b. The condition of continuity for oxygen at z_b gives again a relation between F_c, z_o and O_{bw}:

$$\gamma\phi D_s(O_{bw} - E) = \omega^2 C_{z_b}/k_2 - (k/\beta^2)\,(C_{z_b} - A - B) + rF_c. \tag{5}$$

Figure 8 displays the values of z_o predicted by the model (equations (4) and (5) for $z < z_b$ and $z > z_b$ respectively) together with the experimental values of z_o from the Sulu Sea. It can be expected that both k and K decreases with increasing water depth. As no experimental data is available, their ratio (β^2) was taken as constant over the range of water depths.

The model explains well the gradual increase of z_o with increasing water depth. In the model, the only supply of organic matter is from pelagic sedimentation. Terrigenous supply, which certainly plays a role in this basin, is thus neglected. Figure 8 shows two cores where advective transport leads to an anomalous oxygen penetration. In cores 17 and 18 (both 4500 m) from the Sulu Sea, z_o is only 1 cm instead of the expected 30 cm. In the deep central

PHILOSOPHICAL TRANSACTIONS OF THE ROYAL SOCIETY A MATHEMATICAL, PHYSICAL & ENGINEERING SCIENCES

Sulu Sea, sediment is supplied by turbidites from the eastern slopes of the basin (Exon *et al.* 1981), causing a high accumulation rate of sediments with a high organic carbon content, and a correspondingly high oxygen consumption. A similar situation occurs in the northeastern Atlantic site, where z_o increases with decreasing water depth (figure 2). This anomalous behaviour can be explained by winnowing of the sediment at local highs, resulting in a net downslope transport of fine particles and organic-rich aggregates, and an increased sediment accumulation rate with increasing water depth; the shallow oxygen penetration in the Porcupine Abyssal Plain to the east of this site (core T84-21B) is again related to the presence of turbidites (Rutgers van der Loeff & Lavaleye 1986).

The model predicts a strong increase in sensitivity of z_o on organic input (and consequently on water depth) when oxygen breaks through the bioturbated layer. A finite $z_o > z_b$ is only possible when the supply of oxygen nearly balances the supply of organic carbon. A small change is then sufficient to deplete carbon before oxygen. z_o must be equally sensitive to changes in the supply of oxygen, i.e. in O_{bw}. This is indeed observed in three cores from similar water depth, but from basins with different oxygen concentrations in their bottom waters (figure 9). In the Sulu Sea core ($O_{bw} = 55$ μM), oxygen is depleted at 6 cm. In the South China Sea ($O_{bw} = 105$ μM), oxygen is not depleted until 14 cm, whereas in the western equatorial Pacific ($O_{bw} = 150$ μM) 50 μM O_2 is still present at 20 cm depth, and oxygen is probably not depleted within the first metre.

These experimental data are compared in figure 8 with model predictions by changing only the value of O_{bw} (and correcting D for the different temperature). All other parameters are unchanged. Although the three basins are not far apart, they differ in proximity to the continent and in sediment accumulation rate, and differences in β (Emerson *et al.* 1985) and in primary production rate are also likely. Nevertheless it is remarkable that the change in O_{bw} alone is sufficient to account for the large observed differences in oxygen penetration.

Conclusions

The depth where oxygen is depleted determines the onset of manganese reduction. Indirectly, the depletion of oxygen has implications for the mobility of many trace elements. As manganese oxyhydroxides offer strong adsorption sites, they accumulate a range of other elements during their formation and transit through the aerobic layer. The reductive dissolution of these hydrous oxides sets all associated elements free. This results in the formation of new bonds (trace metals, REE) and to changes in mobility (Mn, Co, Fe, Ni, Cu, and possibly also REE).

The carbon oxidation model developed here shows the sensitivity of the steady-state depth of oxygen depletion z_o to changes in the supply of organic matter or the oxygen concentration in the bottom water. This sensitivity increases when oxygen breaks through the bioturbated zone. The strong dependence of z_o on bottom water oxygen has interesting implications.

First, the higher oxygen concentration in Atlantic bottom water compared with the Pacific favours a deeper oxygen penetration in Atlantic sediments. In contrast, Müller *et al.* (1988) argued that the higher sediment accumulation rates and the resulting higher proportion of carbon that is buried in the Atlantic compared to the Pacific ocean has the opposite effect. This paper gives examples from both oceans, where sediments far enough from productive areas or from continental influences including turbidites, are entirely oxygenated.

Second, an increase in the oxygen concentration of deep-ocean water in the order of 140 μM,

as has probably occurred after the last glaciation (Broecker & Peng 1982), has a dramatic effect on the steady-state z_0 under otherwise identical conditions. This mechanism adds to the downward migration of the oxidation front resulting from the post-glacial decrease in sedimentation rate or a drop in fertility, and must have influenced the cycling of manganese and the conditions for benthic life in sediments throughout the world oceans.

This paper describes samples collected during expeditions with M. S. *Tyro*, H. Ms. *Tydeman*, R. V. *Polarstern* and R. V. *Moana Wave*. I am grateful for the support given by the captains, commander and crews of these ships and by many colleagues on board. Assistance was obtained from D. A. Waijers, C. M. Oomens-Meeuwsen, R. T. P. de Vries, M. Schlüter, S. Wiebe-Kawaletz, G. Kattner and T. Rathburn. The manuscript benefitted from comments of H. de Baar on an earlier version. I thank B. Corliss for the opportunity to take part in the Sulu Sea expedition. The northeastern Atlantic study was supported by the Commission of the European Communities (contracts BIO-B-509-NL (N) and B16-54-NL). Sample collection with R. V. *Moana Wave* was supported by NSF grants OCE-8700744 and OCE-8614128.

References

Aller, R. C. 1988 In *Nitrogen cycling in coastal marine environments* (ed. T. H. Blackburn & J. Sørensen), ch. 13, pp. 301–338. Wiley & Sons.
Andrews, D. & Bennett, A. 1981 *Geochim. cosmochim. Acta* **45**, 2169–2175.
Bennekom, A. J. v. & Berger, G. W. 1984 *Neth. J. Sea Res.* **17**, 149–200.
Berger, W. H., Finkel, R. C., Killingley, J. S. & Marchig, V. 1983 *Nature, Lond.* **303**, 231–233.
Berner, R. A. 1980 *Early diagenesis. A theoretical approach*. Princeton University Press. (241 pages.)
Boyle, E. A. 1983 *Geochim. cosmochim. Acta* **47**, 1815–1819.
Broecker, W. S. & Peng, T.-H. 1982 *Tracers in the sea*. Lamont-Doherty Geol. Obs., Columbia University. (690 pages.)
Burdige, D. J. & Gieskes, J. M. 1983 *Am. J. Sci.* **283**, 29–47.
Callender, E. & Bowser, C. J. 1980 *Am. J. Sci.* **280**, 1063–1096.
Danielsson, L.-G., Magnusson, B. & Westerlund, S. 1979 *Analytica chim. Acta* **98**, 47–57.
De Baar, H. J. W., German, C. R., Elderfield, H. & Van Gaans, P. 1988 *Geochim. cosmochim. Acta* **52**, 1203–1219.
Elderfield, H. & Sholkovitz, E. R. 1987 *Earth planet. Sci. Lett.* **82**, 280–288.
Emerson, S., Fischer, K., Reimers, C. & Heggie, D. 1985 *Deep Sea Res.* **32**, 1–21.
Exon, N. F., Haake, F.-W., Hartmann, M., Kögler, F.-C., Müller, P. J. & Whiticar, M. J. 1981 *Mar. Geol.* **39**, 165–195.
Fischer, G., Fütterer, D., Gersonde, R., Honjo, S., Osterman, D. & Wefer, G. 1988 *Nature, Lond.* **335**, 426–428.
Froelich, P. N., Klinkhammer, G. P., Bender, M. L., Luedtke, N. A., Heath, D. C. & Dauphin, P. 1979 *Geochim. cosmochim. Acta* **43**, 1075–1090.
Gendron, A., Silverberg, N., Sundby, B. & Lebel, J. 1986 *Geochim cosmochim. Acta* **50**, 741–747.
Goloway, F. & Bender, M. 1982 *Limnol. Oceanogr.* **27**, 624–638.
Gust, G., Booij, K., Helder, W. & Sundby, B. 1987 *Neth. J. Sea Res.* **21**, 255–263.
Hartmann, M. & Müller, P. J. 1982 In *The dynamic environment of the ocean floor* (ed. K. A. Fanning & F. T. Mannheim), pp. 285–301. Lexington.
Hartmann, M., Müller, P. J., Suess, E. & van der Weijden, C. H. 1976 *Meteor. Forsch.-Ergebn.* C **24**, 1–67.
Heggie, D. & Lewis, T. 1984 *Nature, Lond.* **311**, 453–455.
Heggie, D., Kahn, D. & Fischer, K. 1986 *Earth planet. Sci. Lett.* **80**, 106–116.
Helder, W. & Bakker, J. F. 1985 *Limnol. Oceanogr.* **30**, 1106–1109.
Jahnke, R., Heggie, D., Emerson, S. & Grundmanis, V. 1982 *Earth planet. Sci. Lett.* **61**, 233–256.
Klinkhammer, G. P. 1980 *Earth planet. Sci. Lett.* **49**, 81–101.
Klinkhammer, G. P., Heggie, D. T. & Graham, D. W. 1982 *Earth planet. Sci. Lett.* **61**, 211–219.
Lebel, J., Silverberg, N. & Sundby, B. 1982 *Deep Sea Res.* **29**, 1365–1372.
Lyle, M. 1983 *Limnol. Oceanogr.* **28**, 1026–1033.
Lyle, M., Heath, G. R. & Robbins, J. M. 1984 *Geochim. cosmochim. Acta* **48**, 1705–1715.
Lynn, D. C. & Bonatti, E. 1965 *Mar. Geol.* **3**, 457–474.
Martin, W. R. 1985 *Transport of trace metals in nearshore sediments*. Thesis, Woods Hole Oceanographic Institute, Massachusetts, U.S.A.
Müller, P. J., Hartmann, M. & Suess, E. 1988 In *The manganese nodule belt of the Pacific Ocean* (ed. P. Halbach, G. Friedrich & U. v. Stackelberg), pp. 70–90. Stuttgart: Ferdinand Enke.

PHILOSOPHICAL TRANSACTIONS OF THE ROYAL SOCIETY A MATHEMATICAL, PHYSICAL & ENGINEERING SCIENCES

Müller, P. J. & Mangini, A. 1980 *Earth planet. Sci. Lett.* **51**, 94–114.
Murray, J. W. & Dillard, J. G. 1979 *Geochim. cosmochim. Acta* **43**, 781–787.
Murray, J. W. & Grundmanis, V. 1980 *Science, Wash.* **209**, 1527–1530.
NEA 1985 *Review of the continued suitability of the dumping site for radioactive waste in the North-East Atlantic* OECD, Paris, 448 pp.
Pedersen, T. F., Vogel, J. S. & Southon, J. R. 1986 *Geochim. cosmochim. Acta* **50**, 2019–2031.
Reimers, C. E. 1987 *Deep Sea Res.* **34**, 2019–2035.
Reimers, C. E., Kalhorn, S., Emerson, S. R. & Nealson, K. H. 1984 *Geochim. cosmochim. Acta* **48**, 903–910.
Revsbech, N. P. 1989 *Limnol. Oceanogr.* **34**, 474–478.
Revsbech, N. P., Jørgensen, B. B. & Blackburn, T. H. 1980 *Science, Wash.* **207**, 1355–1356.
Rutgers van der Loeff, M. M. & Bennekom, A. J. v. 1989 *Deep Sea Res.* **36**, 1341–1357.
Rutgers van der Loeff, M. M. & Lavaleye, M. S. S. 1986 *Sediments, fauna and the dispersal of radionuclides at the N.E. Atlantic dumpsite for low-level radioactive waste.* Texel: Netherlands Institute for Sea Research. (134 pages.)
Sørensen, J. & Wilson, T. R. S. 1984 *Limnol. oceanogr.* **29**, 650–652.
Sayles, F. L. 1981 *Geochim. cosmochim. Acta* **45**, 1061–1086.
Suess, E. 1976 In *The benthic boundary layer* (ed. J. N. McCave), pp. 57–79. New York: Plenum Press.
Suess, E. 1980 *Nature, Lond.* **288**, 260–263.
Sundby, B., Anderson, L. G., Hall, P. O., Iverfeldt, A., Rutgers van der Loeff, M. M. & Westerlund, S. F. G. 1986 *Geochim. cosmochim. Acta* **50**, 1281–1288.
Wallace, H. E., Thomson, J., Wilson, T. R. S., Weaver, P. P. E., Higgs, N. C. & Hydes, D. J. 1988 *Geochim. cosmochim. Acta* **52**, 1557–1569.
Westerlund, S. F. G., Anderson, L. G., Hall, P. O., Iverfeldt, A., Rutgers van der Loeff, M. M. & Sundby, B. 1986 *Geochim. cosmochim. Acta* **50**, 1289–1296.
Wilson, T. R. S., Thomson, J., Colley, S., Hydes, D. J., Higgs, N. C. & Sørensen, J. 1985 *Geochim. cosmochim. Acta* **49**, 811–822.
Wilson, T. R. S., Thomson, J., Hydes, D. J., Colley, S., Culkin, F. & Sørensen, J. 1986 *Science, Wash.* **232**, 972–975.

Discussion

P. S. Meadows (*Department of Zoology, Glasgow, U.K.*). Firstly, bioturbation usually extends well below 8 cm in most sediments unless they are very anoxic inshore ones, and secondly bioturbation rarely stops suddenly; it is more usual for it to decay in an approximately exponential fashion. Can Dr Rutgers van der Loeff comment on these points, please, in relation to his modelling?

M. M. Rutgers van der Loeff. Open burrows have been observed to much greater depths than 8 cm in deep-sea sediments, but the presence of burrows does not imply a significant mixing rate to those depths. Mixing rates have been determined in many deep-sea sediments using a variety of tracers with different timescales. The data indicate appreciable mixing in the upper 6–8 cm of deep-sea sediments. Below, mixing rates are much lower, but certainly bioturbation decreases gradually with depth. A stepwise decay was chosen for simplicity. When appropriate data on bioturbation rates are available for a certain sediment, the bioturbation function in the model could be refined. The solution would then require numerical modelling.

J. A. Allen (*University Marine Biological Station, Millport, Isle of Cumbrae, U.K.*). In Dr Rutgers van der Loeff's comparisons of the results from the Sulu Sea with those in the Atlantic, did he take into account the differences in bottom water temperatures? I believe that that of the Sulu Sea is approximately 10 °C as compared with about 2.5 °C for the Atlantic stations at similar depths.

M. M. Rutgers van der Loeff. Yes, the diffusion coefficients were corrected for temperature.